Catalysis Science & Technology

PAPER

View Article Online
View Journal | View Issue

Check for updates

Cite this: Catal. Sci. Technol., 2024, 14, 3699

A cobalt molecular catalyst for hydrogen evolution reaction with remarkable activity in phosphate buffered water solution†

Caterina Trotta,[a] Pardeep Dahiya,[b] Lorenzo Baldinelli, [a] Gabriel Menendez Rodriguez, *[a] Priyanka Chakraborty,[b] Giovanni Bistoni, *[a] Filippo De Angelis,[a] Basker Sundararaju *[b] and Alceo Macchioni *[a]

Received 15th February 2024,
Accepted 28th May 2024

DOI: 10.1039/d4cy00209a

rsc.li/catalysis

Herein, we show that [Cp*Co(2-ampy)I]I (2-ampy = 2-aminomethyl-pyridine) is an extremely active catalyst for HER, exhibiting a TOF of 109 000 s^{-1} in phosphate buffered water solution (pH 7). The key to this remarkable activity stems from the establishment of a network of weak interactions in the second coordination sphere. As a matter of fact, both experimental and theoretical studies strongly suggest that the $-NH_2$ functionality of the 2-ampy ligand acts as an anchoring and orienting group for $H_2PO_4^-$ through the establishment of an intermolecular hydrogen bonding with it that, in turn, intermolecularly donates a proton to Co–H liberating H_2.

The production of green hydrogen by renewable energy-powered water electrolysis is considered a viable solution to the problems of fossil solar-fuels depletion and the dramatic environmental consequences of their massive use.[21–24] Catalysis plays an essential role in the realization of an efficient electrolysis apparatus making it possible to minimize the energy expenditure required, close to that established by thermodynamics, for both reductive and oxidative processes.[25–29] With regard to the hydrogen evolution reaction (HER) significant advances have been achieved in the identification of molecular catalysts based on earth-abundant metals, such as iron,[30–32] cobalt,[33–38] nickel,[39–42] copper[43,44] and molybdenum.[45,46] Several key factors contributing to improve HER catalysis have been identified.[47–55] It has been understood that having a hanging functionality acting as proton source in the proximity of the metal active site is essential to facilitate the protonation of the M–H intermediate, thus leading to H_2 evolution (D–H⋯H–M, Scheme 1a). This is exactly what occurs in [Fe,Fe] or [Ni,Fe] hydrogenases,[56–59] which efficiently catalyze the reduction of protons to H_2 [turnover frequency (TOF) values up to *ca.* 10^4 s^{-1}], where an –NH moiety of the thiolate bridging ligand is responsible for intramolecularly relaying the proton from the external source to the M–H fragment. This teaching of Nature inspired the development of many mono- and dinuclear complexes, having a basic group in the second coordination sphere, as structural and functional models of hydrogenase.[39,60–68] For instance, Rauchfuss and co-workers demonstrated that the presence of a pendant amine, in a structural model of [Fe,Fe] hydrogenase, enhances the HER

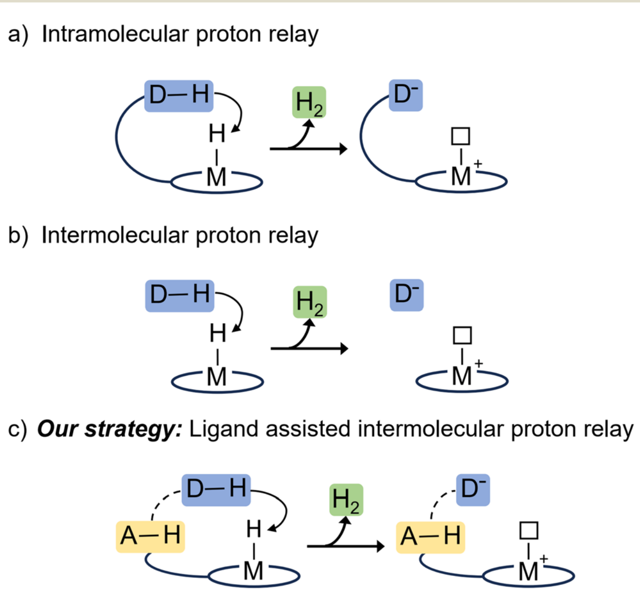

Scheme 1 Second coordination sphere proton relay processes (a–c) facilitating HER catalysis (M = transition metal, D–H = proton donor, A–H = anchoring group).

[a] Department of Chemistry, Biology and Biotechnology and CIRCC, Università degli Studi di Perugia, Via Elce di Sotto 8, 06123-Perugia, Italy. E-mail: gabriel.menendezrodriguez@unipg.it, giovanni.bistoni@unipg.it, alceo.macchioni@unipg.it

[b] Department of Chemistry, Indian Institute of Technology Kanpur, 208 016 Kanpur, Uttar Pradesh, India. E-mail: basker@iitk.ac.in

† Electronic supplementary information (ESI) available: The authors have cited additional references within the supporting information.[1–20] CCDC 1939352 and 2297771. For ESI and crystallographic data in CIF or other electronic format see DOI: https://doi.org/10.1039/d4cy00209a

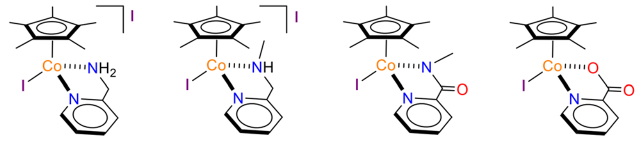

1 2 3 4

Scheme 2 Structure of cobalt complexes.

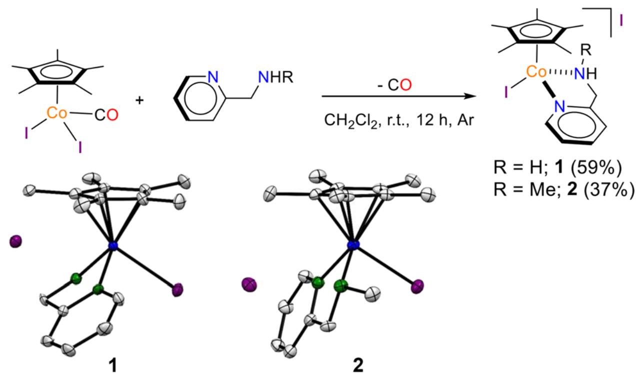

Scheme 3 Synthesis of cobalt complexes **1** and **2** (ORTEP diagram of complexes with thermal ellipsoids are shown at the 50% probability level, H atoms are omitted for clarity).

rate.[69] DuBois and co-workers reported a nickel complex $[Ni(PPh_2NPh)_2](BF_4)_2$, (PPh2NPh = 1,3,6-triphenyl-1-aza-3,6-diphosphacycloheptane) with remarkable activity (TOF = 106 000 s^{-1}, in acetonitrile with 1.2 M of water) in HER attributed to the key role played by a pendant amine acting as intramolecular proton relay.[39] Analogously, Nocera and co-workers showed that the presence of a carboxylic acid hanging group of a cobalt "hangman" porphyrin facilitates HER by mediating, intramolecularly, a proton-coupled electron transfer (PCET) process.[66–68]

Interestingly, there are now some pieces of evidence clearly indicating that HER reaction can be also facilitated by intermolecular protonation (D–H⋯H–M, Scheme 1b). Particularly, Bren and co-workers recently reported insightful studies on the effects of pK_a and buffer nature on the activity of cobalt-based catalysts.[70–72] They found an acceleration of HER rates of 2 to 4 orders of magnitude moving from water to buffered water solution, at the same pH, demonstrating an active role of the buffer as a proton donor. Sakai and co-workers attributed the remarkable activity of a cobalt catalyst with a pentadentate macrocyclic ligand in HER to the key role played by $H_2PO_4^-$ derived from the phosphate buffer as a proton source.[73]

Herein, we show that [Cp*Co(2-ampy)I]I (2-ampy = 2-aminomethyl-pyridine; **1**, Scheme 2) is an extremely active catalyst for HER exhibiting a remarkable TOF of 109 000 s^{-1} in phosphate buffered water solution (PBS, pH 7). Mechanistic studies suggest that the key to success of **1** lies in the occurrence of a crucial hydrogen bond network in the second coordination sphere: the $-NH_2$ functionality of the 2-ampy ligand acts as an anchoring and orienting group for $H_2PO_4^-$ through the establishment of an intermolecular hydrogen bonding with it, which, in turn, donates a proton to the M–H group (D–H⋯A–H⋯H–M, Scheme 1c).[74] This hypothesis has been supported by i) contrasting the electrocatalytic performances of **1** to those of selected members of the novel family of potentially active [Cp*CoL$_3$] catalysts (Scheme 2), deliberately turning of or altering the crucial intermolecular hydrogen bonds by a proper choice of the bidentate ligand; ii) in depth quantum DFT calculations aimed at understanding the ligand effect on the catalytic performance implicitly taking into account the interactions with the buffer.

Novel complexes **1** and **2** were synthesized by the reaction of Cp*Co(CO)I$_2$ (ref. 75) with commercially available inexpensive 2-ampy and characterized both in solution and in the solid state (ESI†) (Scheme 3). Complexes **3** (ref. 76) and **4** (ref. 77) were reported by one of us and prepared as per the procedure described.

Complexes **1–4** were characterized electrochemically by cyclic voltammetry (CV) and square wave voltammetry (SWV) (Fig. 1). Each compound displays a redox event in the −0.2 and −0.5 V potential range attributed to the $Co^{III/II}$ reduction. Peak current *versus* square root of scan rate is always linear, indicating a diffusional nature of the process (Fig. S2–S5†).

As shown in Table 1, the half-wave potential ($E_{1/2}$) and redox behavior of the Co^{III}/Co^{II} couple of **1–4** are sensitive to the nature of the ligand coordinated at the Cp*Co moiety. **1–2** show a quasi-reversible reduction as indicated by the

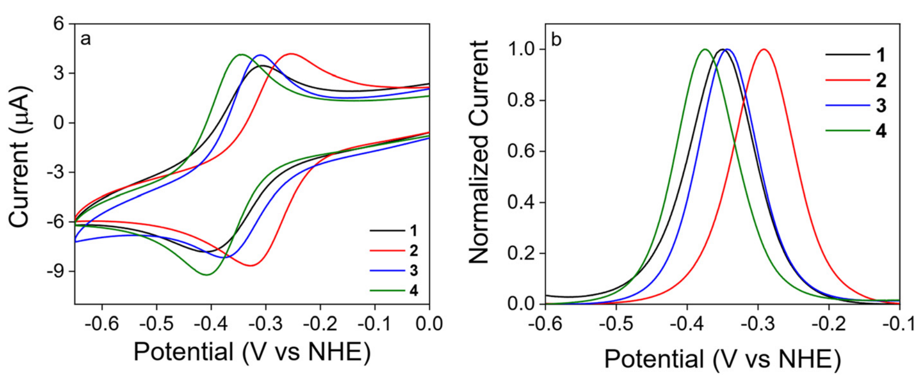

Fig. 1 a) CVs of **1–4** (500 μM) at 100 mV s^{-1} scan rate and b) SWVs of **1–4** (500 μM) recorded in 0.1 M PBS at pH 7 under N_2.

Table 1 Cyclic voltammetry data for **1–4**

Complex	$E_{1/2}$ (V)	ΔE_p (mV)	i_{ox}/i_{red}
1	−0.350	95.2	0.93
2	−0.292	88.2	0.89
3	−0.345	65.9	1.49
4	−0.375	64.1	1.01

Table 2 HER electrocatalytic data for **1–4**

Complex	i_{cat}/i_d	$\eta(E_{cat/2})$ (V)	TOF (s^{-1})
1	136	1.034	39 000 ± 3000
2	77	0.964	16 000 ± 2500
3	10	0.635	900 ± 50
4	15	0.689	2000 ± 250

large peak-to-peak separation (ΔE_p), with a peak current ratio (i_{ox}/i_{red}) nearly one. Notably, a positive shift of 58 mV is observed when comparing the $E_{1/2}$ of **1** (−0.350 V) to that of **2** (−0.292 V). Considering the greater electron donation ability of methyl relative to hydrogen, a shift in the opposite direction should be observed suggesting that a different ligand is coordinated at Cp*Co(*N*,*N*) moiety in **1** and **2**.

To validate this possibility, CVs and SWVs of **1** and **2** were recorded in a 0.1 M $NaClO_4$ (pH 7) electrolyte solution instead that in PBS. This led to an anodic shift of 30 mV of the $Co^{III/II}$ redox potential of **1**, while had no (or a negligible) effect on that of **2** (Fig. S6 and S7†), confirming the hypothesis that **1** and **2** in PBS differ in the nature of the third ligand coordinated at Co, which is most likely phosphate in **1** and water in **2**. Consistently, a cathodic shift of $E_{1/2}$ was observed for **1** upon increasing pH (*i.e.* increasing the $HPO_4^{2-}/H_2PO_4^-$ ratio, Fig. S8†).[78,79] The $Co^{III/II}$ redox couple of **3** and **4** are observed at $E_{1/2}$ = −0.345 (ΔE_p = 65.9 mV) and −0.375 V (ΔE_p = 64.1 mV), respectively, indicating the higher electron donor properties of the carboxylate ligand.

At more cathodic potentials, an additional irreversible wave, characterized by a significant current increase, was observed (Fig. 2). It was ascribed to the electrocatalytic hydrogen evolution reaction: $2H^+ + 2e^- \rightarrow H_2$ (HER). H_2 production was confirmed by rotating ring disk electrochemistry (ESI†). **1** and **2** show similar onset potentials (−1.13 V and −1.11 V, respectively). For **2** the catalytic wave is preceded by an irreversible wave that might be ascribed to the transformation of the precatalyst into the active species or the formation of a stable catalytic intermediate.[78,79] **3** and **4** exhibit a considerably more anodic onset potential of −0.88 V and −0.95 V, respectively. As shown in Table 2, the largest current increase (i_{cat}/i_d = 136, where i_{cat} is the maximum catalytic current and i_d is the cathodic peak current of the $Co^{III/II}$ redox couple) was observed for **1**, suggesting an extremely fast catalytic reaction, followed by **2** (i_{cat}/i_d = 77), **4** (i_{cat}/i_d = 15) and **3** (i_{cat}/i_d = 10). Remarkably, moving from **1** to **2**, *i.e.* substituting a hydrogen atom with a methyl group, strongly affects the catalytic activity, causing a decrease of approximately one-half of the i_{cat}/i_d ratio.

Before conducting further mechanistic studies, we investigated whether the electrocatalytic activity of **1–4** was indeed ascribed to the homogeneous catalyst in solution, rather than to any electrocatalytically active species bound to the surface. The possible formation of any deposited species under catalytic conditions was evaluated by continuously recording 50 CV scans from 0.19 to −1.45 V at 1 V s^{-1} scan rate on a 500 μM solution of catalyst. In all cases, the catalytic current at −1.45 V gradually loses intensity as new oxidation waves appear in the −0.7 to 0.2 V potential range (Fig. S13–S16†). This behaviour is consistent with the formation of new deposited species derived from partial catalyst decomposition. The intensity of the $Co^{III/II}$ redox couple of **1–4** also decreased over the same period, further indicating that the surface composition of the glassy carbon electrode was changing. However, the rinse test, performed after 50 scans, clearly shows a negligible activity of the catalyst decomposition products. Controlled-potential electrolysis (CPE) measurements carried out at −1.35 V confirmed the rather short live of the catalytic systems, as well as the substantial inactivity of deposited species, since the recorded current abruptly decreases, reaching the one obtained in the absence of catalyst in less than 3 minutes (Fig. S17†). Exception made for complex **4**, whose

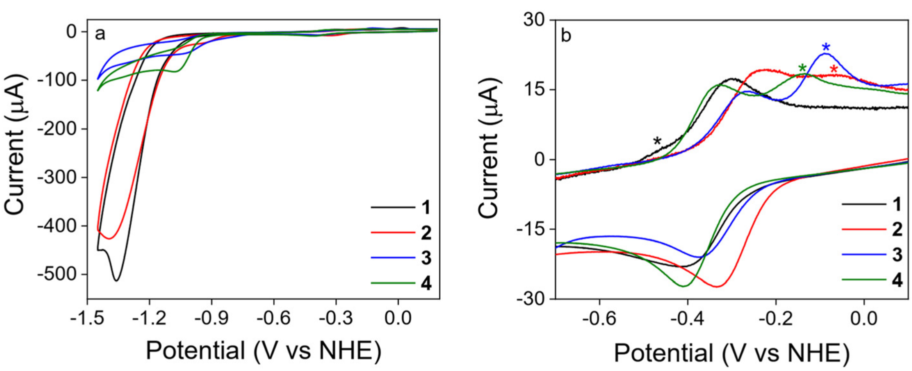

Fig. 2 a) CVs of **1–4** (500 μM) at 100 mV s^{-1} scan rate recorded in 0.1 M PBS at pH 7 under N_2. b) Enlarged view of $Co^{III/II}$ redox region of the first CV of **1–4** (500 μM) recorded at 1 V s^{-1} from 0.19 to −1.45 V in 0.1 M PBS at pH 7 under N_2 (asterisks denote the new oxidation features observed on the return sweep ascribed to catalyst degradation products).

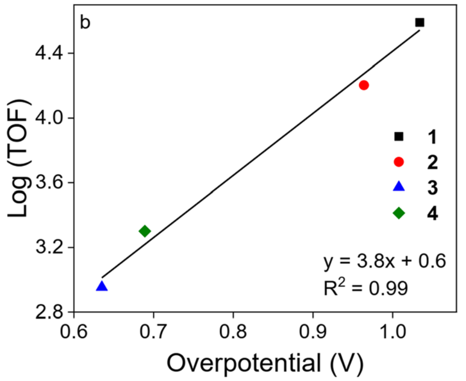

Fig. 3 Plot of Log(TOF) as a function of catalyst overpotential.

degradation somehow leads to a slightly active species (Fig. S17†). It is worth noting that a significant difference was found between **1** and **2–4** in terms of catalyst stability. In particular, the degradation of **2–4** is more pronounced than that of **1**. This can be deduced by the noticeable appearance of new oxidative waves in the first CV of the solution of **2–4**. Unlike **1**, for which additional redox events due to catalyst decomposition are almost negligible (Fig. 2b). This result demonstrates that **1**, not only is the most active catalyst, but also the one that is less prone to degradation. More importantly, it was found that such degradation processes are only relevant in those experiments for which the catalyst is exposed to reductive potentials for a substantial period of time. As a matter of fact, in CV experiments of **1** recorded at high scan rates (>6 V s^{-1}), *i.e.* where the time scale of the experiment is considerably reduced, no sign of degradation is observed (Fig. S18†). Under such conditions, pure catalytic regime is reached, allowing the TOF to be determined.

Considering the above results, to prevent that any deposited species negatively influences the current response of the studied complexes, only the first scan, recorded on a freshly polished electrode, was considered. Moreover, this work focuses only on the evaluation of the activity of the molecular complexes in solution and the related HER mechanism, not on long-term activity since in that case the formation of heterogeneous deposits on the electrode surface cannot be neglected.

In order to benchmark our catalysts, the HER overpotential, $\eta(E_{\mathrm{cat}/2})$,[80,81] and TOF[82,83] of **1–4** were determined (ESI†). As summarized in Table 2, **1–2** operates at higher overpotentials (1.034 and 0.964 V, respectively) than **3–4** (0.635 V and 0.689 V, respectively). Catalysts with somewhat lower overpotential have been reported in the literature.[63,84–86] For **1**, a remarkable TOF of 39 000 s^{-1} was observed (Fig. S20†). Whereas TOF values of 16 000 s^{-1}, 900 s^{-1} and 2000 s^{-1} were obtained for **2**, **3** and **4**, respectively (Fig. S21–S23†). It can be hypothesized that the superior performances of **1** is due to the presence of the $-NH_2$ functionality that binds $H_2PO_4^-$ anion, properly orienting it in a way to facilitate the proton transfer to Co–H (*vide infra*).[87,88] The significant lower activity of **2** compared to **1** is also consistent with such interpretation since having a –NHMe in place of $-NH_2$ clearly disfavors hydrogen bonding

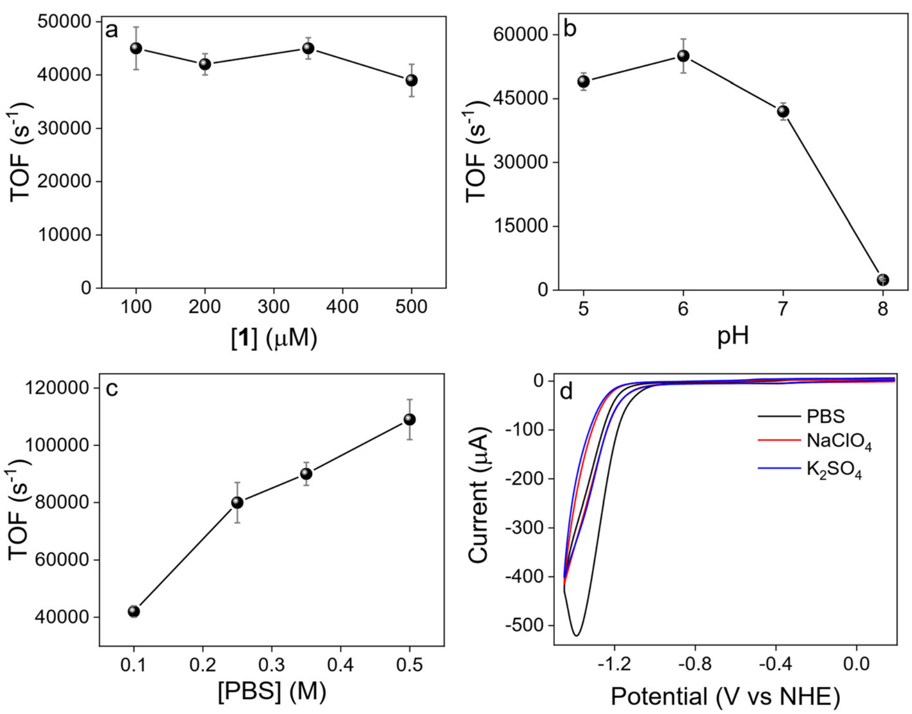

Fig. 4 Dependence of TOF on a) [**1**] (0.1 M PBS at pH 7 under N_2), b) pH ([**1**] = 200 μM, 0.1 M PBS under N_2), and c) [PBS] ([**1**] = 200 μM, pH 7 under N_2). d) CVs of **1** (200 μM) at 100 mV s^{-1} scan rate using PBS (black trace), $NaClO_4$ (red trace) and K_2SO_4 (blue trace) as supporting electrolyte at pH 7 (0.1 M).

with $H_2PO_4^-$, at least statistically. The higher activity of **4** with respect to **3** might be attributed to the greater ability of the former to undergo hydrogen bonding with $H_2PO_4^-$, using the lone pairs of the coordinated carboxylic oxygen atom.

Interestingly, the Log(TOF) *versus* overpotential plot for **1–4** exhibits a nice linear trend (Fig. 3) suggesting that the same reaction mechanism is reasonably active and the structural differences of complexes systematically tune the free energies of intermediates and reaction steps of the catalytic cycle.[89–94] Our DFT computational results are in line with this hypothesis (*vide infra*).

Additional electrochemical mechanistic studies were carried out for **1** exhibiting the highest catalytic performances. TOF remains constant (TOF_{mean} = 42 000 s^{-1}) changing catalyst concentration in the 100–500 μM range (Fig. 4a), consistently with a first order on **1**. By varying the pH of PBS from 5 to 6 does not significantly affect the activity of **1** (TOF = 49 000 ± 2000 s^{-1}, pH 5; TOF = 55 000 ± 4000 s^{-1}, pH 6) (Fig. 4b). However, a further increase of pH leads to a significant decrease of TOF (42 000 ± 2000 s^{-1}, pH 7; 2400 ± 250 s^{-1}, pH 8). This peculiar behavior suggests that H_2 evolution rate might be also influenced by the concentration of $H_2PO_4^-$, whose concentration decreases as pH increases.[38,95–97] To corroborate this hypothesis, electrocatalytic experiments were performed at constant pH varying buffer strength. It was observed a marked increase of TOF with increasing buffer strength (Fig. 4c), up to a value of 109 000 ± 7000 s^{-1}, obtaining another strong hint that $H_2PO_4^-$ plays an active role in hydrogen evolution, likely acting as proton source. Consistently, a significantly lower current was observed using $NaClO_4$ or K_2SO_4 as supporting electrolytes instead of PBS (Fig. 4d).

The experimental results reported above were complemented by extensive DFT computational studies for **1** (Fig. 5) and **3** (as reference, ESI†) aimed at providing insights into the mechanistic aspects of HER catalysis, focusing on understanding the intimate reason why **1** exhibit such a remarkable activity. Our results indicate that HER catalysis by **1** and **3** follows the same reaction mechanism (Fig. 5a and S33†), which is consistent with the observed scaling relationships for these catalysts. In the first step, **[Co(III)–H]**$^{+n}$ [where **Co** = Cp*Co(*N*,*N*)] forms through a PCET pathway by far at lower energy (+0.95 eV for **1** and +0.78 eV for **3**) compared to the two-step reduction-protonation counterpart (+1.66 eV for **1** and +1.58 eV for **3**). Importantly, the calculated energy associated to the formation of the hydride species of **3** (0.78 eV), which is responsible for the measured overpotential, is significantly lower than that of **1** (0.95 eV). This trend nicely correlates with the experimentally measured overpotentials of **1** and **3**, which amounts to 1.03 V and 0.63 V, respectively. Once **[Co(III)–H]**$^{+n}$ is formed, the presence of the phosphate becomes crucial for the HER catalytic mechanism. It was found that the most favorable pathway for H_2 generation involves the coordination of $H_2PO_4^-$ in the second sphere of **[Co(III)–H]**$^{+n}$ resulting in the formation of the key intermediate **[Co(III)–H]**$^{+n}$**(**$H_2PO_4^-$**)**. It is in this context that the difference between **1** and **3** appear the most.

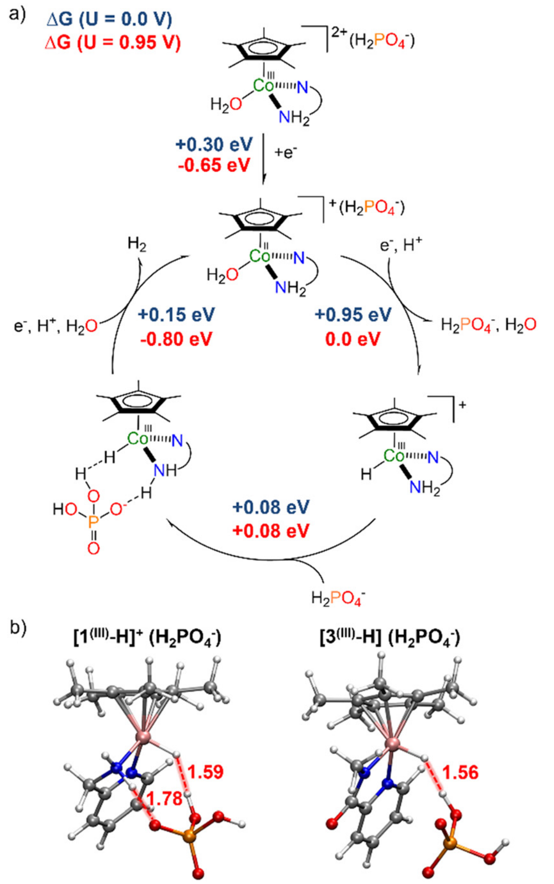

Fig. 5 a) Proposed catalytic HER cycle for 1 and energetics at 0.0 V (blue) and 0.95 V (red). At potentials higher than 0.95 V, all steps involving an electron transfer from the electrode become exergonic. b) DFT-optimized structures for **[1(III)–H]**$^+$**(**$H_2PO_4^-$**)** and **[3(III)–H](**$H_2PO_4^-$**)**. Hydrogen-bond distances are reported in Å.

The optimized **[Co(III)–H]**$^{+n}$$H_2PO_4^-$ structures shown in Fig. 5b, reveal that while a strong **Co–H···HOPO**$_3$**H** dihydrogen bond[98,99] is present both in **1** (distance = 1.59 Å) and **3** (distance = 1.56 Å), a strong $–NH_2···OPO_3H^-$ establishes in **1** (distance = 1.78 Å). The cooperativity of those two types of H-bonding in **1** contributes to a more facile association of $H_2PO_4^-$ in the second coordination sphere in **1** (+0.08 eV) than in **3** (+0.29 eV), thus favoring hydrogen donation. Once $H_2PO_4^-$ is in the second coordination sphere, the kinetic barrier to transfer a proton to Co–H is almost zero for both **1** and **3**, and the increase of energy passing from **[Co(III)–H]**$^{+n}$**(**$H_2PO_4^-$**)** to **[Co(III)–OH**$_2$**]**$^{+n}$ and H_2, through a PCET pathway, is similar (+0.15 eV for **1**, +0.12 eV for **3**; ESI†).

In conclusion, we have reported some molecular cobalt catalysts highly active in hydrogen evolution reaction. Particularly, complex [Cp*Co(2-ampy)I]I **1**, whose second coordination sphere was rationally designed for having a $–NH_2$ moiety that attracts and orients $H_2PO_4^-$ of the buffer, which, in turn, acts as proton donor to the metal hydride functionality, exhibits extremely high TOF (109 000 s^{-1}), importantly, working in water exclusively. To the best of our knowledge, only an organometallic [2Fe–2S] mimic of the active site of an [FeFe]-hydrogenase enzyme shows considerably higher TOF in water solution (250 000 s^{-1}).[65] Considering that **1** belongs to a broad class of compounds, we believe that a rational design of the ancillary ligands, not only in terms of desired electronic and steric features but also of proper functionalities in the second coordination sphere, will likely lead to the discovery of other catalysts with even better performances.

Conflicts of interest

There are no conflicts to declare.

Acknowledgements

This work has been funded by the European Union NextGenerationEU under the Italian Ministry of University and Research (MUR) National Innovation Ecosystem grant ECS00000041 VITALITY. BS acknowledge SERB (CRG/2020/001282) for to support this re-search. PD and PC thank CSIR and IITK for their fellowship. BS thanks Dr. Manoj K. Gangwar for initial study in isolation of these complexes. We acknowledge Università degli Studi di Perugia and MUR for support within the project Vitality, Progetti Fondo Ricerca di Ateneo 2021 and PON Ricerca e Innovazione DM 1062 (J91B21003250006). We also thank the Fondazione Perugia (project 21101, 2022.0405) for supporting our research.

References

1 E. Higuchi, H. Uchida and M. Watanabe, *J. Electroanal. Chem.*, 2005, **583**, 69–76.
2 Y. Bao, K. Nagasawa, Y. Kuroda and S. Mitsushima, *Electrocatalysis*, 2020, **11**, 301–308.
3 J. G. Vos and M. T. M. Koper, *J. Electroanal. Chem.*, 2019, **850**, 113363.
4 J. Zheng, Y. Yan and B. Xu, *J. Electrochem. Soc.*, 2015, **162**, F1470–F1481.
5 S. K. M. Padavala and K. A. Stoerzinger, *ACS Catal.*, 2023, **13**, 4544–4551.
6 Q. Wang, J. Guo and P. Chen, *Joule*, 2020, **4**, 705–709.
7 F. Neese and J. Wiley, *Wiley Interdiscip. Rev.: Comput. Mol. Sci.*, 2012, **2**, 73–78.
8 A. D. Becke, *J. Chem. Phys.*, 1993, **98**, 1372–1377.
9 C. Lee, W. Yang and R. G. Parr, *Phys. Rev. B: Condens. Matter Mater. Phys.*, 1988, **37**, 785.
10 P. J. Stephens, F. J. Devlin, C. F. Chabalowski and M. J. Frisch, *J. Phys. Chem.*, 1994, **98**, 11623–11627.
11 S. Grimme, J. Antony, S. Ehrlich and H. Krieg, *J. Chem. Phys.*, 2010, **132**, DOI: 10.1063/1.3382344.
12 S. Grimme, *Wiley Interdiscip. Rev.: Comput. Mol. Sci.*, 2011, **1**, 211–228.
13 F. Weigend and R. Ahlrichs, *Phys. Chem. Chem. Phys.*, 2005, **7**, 3297–3305.
14 V. Barone and M. Cossi, *J. Phys. Chem. A*, 1998, **102**, 1995–2001.
15 M. Cossi, N. Rega, G. Scalmani and V. Barone, *J. Comput. Chem.*, 2003, **24**, 669–681.
16 G. Henkelman and H. Jónsson, *J. Chem. Phys.*, 2000, **113**, 9978–9985.
17 G. Henkelman, B. P. Uberuaga and H. Jónsson, *J. Chem. Phys.*, 2000, **113**, 9901–9904.
18 S. Trasatti, *Pure Appl. Chem.*, 1986, **58**, 955–966.
19 I. A. Topol, G. J. Tawa, S. K. Burt and A. A. Rashin, *J. Chem. Phys.*, 1999, **111**, 10998–11014.
20 M. D. Tissandier, K. A. Cowen, W. Y. Feng, E. Gundlach, M. H. Cohen, A. D. Earhart, J. V. Coe and T. R. Tuttle, *J. Phys. Chem. A*, 1998, **102**, 7787–7794.
21 J. A. Turner, *Science*, 2004, **305**, 972–974.
22 R. Eisenberg and D. G. Nocera, *Inorg. Chem.*, 2005, **44**, 6799–6801.
23 T. R. Cook, D. K. Dogutan, S. Y. Reece, Y. Surendranath, T. S. Teets and D. G. Nocera, *Chem. Rev.*, 2010, **110**, 6474–6502.
24 N. Armaroli and V. Balzani, *Angew. Chemie Int. Ed.*, 2007, **46**, 52–66.
25 S. Berardi, S. Drouet, L. Francàs, C. Gimbert-Suriñach, M. Guttentag, C. Richmond, T. Stoll and A. Llobet, *Chem. Soc. Rev.*, 2014, **43**, 7501–7519.
26 G. Menendez Rodriguez and A. Macchioni, *Eur. J. Inorg. Chem.*, 2023, **26**, e202200625.
27 W. T. Eckenhoff, *Coord. Chem. Rev.*, 2018, **373**, 295–316.
28 B. Zhang and L. Sun, *Chem. Soc. Rev.*, 2019, **48**, 2216–2264.
29 F. Zaccaria, G. Menendez Rodriguez, L. Rocchigiani and A. Macchioni, *Front. Catal.*, 2022, **2**, 892183.
30 R. Mejia-Rodriguez, D. Chong, J. H. Reibenspies, M. P. Soriaga and M. Y. Darensbourg, *J. Am. Chem. Soc.*, 2004, **126**, 12004–12014.
31 F. Quentel, G. Passard and F. Gloaguen, *Energy Environ. Sci.*, 2012, **5**, 7757–7761.
32 Y. Na, M. Wang, K. Jin, R. Zhang and L. Sun, *J. Organomet. Chem.*, 2006, **691**, 5045–5051.
33 Y. Sun, J. P. Bigi, N. A. Piro, M. L. Tang, J. R. Long and C. J. Chang, *J. Am. Chem. Soc.*, 2011, **133**, 9212–9215.
34 K. M. Waldie, S. K. Kim, A. J. Ingram and R. M. Waymouth, *Eur. J. Inorg. Chem.*, 2017, **2017**, 2755–2761.
35 W. M. Singh, T. Baine, S. Kudo, S. Tian, X. A. N. Ma, H. Zhou, N. J. DeYonker, T. C. Pham, J. C. Bollinger, D. L. Baker, B. Yan, C. E. Webster and X. Zhao, *Angew. Chem.*, 2012, **124**, 6043–6046.
36 A. Call, F. Franco, N. Kandoth, S. Fernández, M. González-Béjar, J. Pérez-Prieto, J. M. Luis and J. Lloret-Fillol, *Chem. Sci.*, 2018, **9**, 2609–2619.
37 C. R. Carr, A. Taheri and L. A. Berben, *J. Am. Chem. Soc.*, 2020, **142**, 12299–12305.
38 J. W. Wang, K. Yamauchi, H. H. Huang, J. K. Sun, Z. M. Luo, D. C. Zhong, T. B. Lu and K. Sakai, *Angew. Chemie Int. Ed.*, 2019, **58**, 10923–10927.
39 M. L. Helm, M. P. Stewart, R. M. Bullock, M. R. DuBois and D. L. DuBois, *Science*, 2011, **333**, 863–866.

40 L. Gan, T. L. Groy, P. Tarakeshwar, S. K. S. Mazinani, J. Shearer, V. Mujica and A. K. Jones, *J. Am. Chem. Soc.*, 2015, **137**, 1109–1115.
41 O. R. Luca, S. J. Konezny, J. D. Blakemore, D. M. Colosi, S. Saha, G. W. Brudvig, V. S. Batista and R. H. Crabtree, *New J. Chem.*, 2012, **36**, 1149–1152.
42 E. S. Wiedner, A. M. Appel, S. Raugei, W. J. Shaw and R. Morris Bullock, *Chem. Rev.*, 2022, **122**, 12427–12474.
43 D. Khusnutdinova, B. L. Wadsworth, M. Flores, A. M. Beiler, E. A. Reyes Cruz, Y. Zenkov and G. F. Moore, *ACS Catal.*, 2018, **8**, 9888–9898.
44 P. Zhang, M. Wang, Y. Yang, T. Yao and L. Sun, *Angew. Chemie Int. Ed.*, 2014, **53**, 13803–13807.
45 H. I. Karunadasa, C. J. Chang and J. R. Long, *Nature*, 2010, **464**, 1329–1333.
46 H. I. Karunadasa, E. Montalvo, Y. Sun, M. Majda, J. R. Long and C. J. Chang, *Science*, 2012, **335**, 698–702.
47 K. Koshiba, K. Yamauchi and K. Sakai, *Angew. Chemie Int. Ed.*, 2017, **56**, 4247–4251.
48 B. D. Stubbert, J. C. Peters and H. B. Gray, *J. Am. Chem. Soc.*, 2011, **133**(45), 18070–18073.
49 H. Lei, A. Han, F. Li, M. Zhang, Y. Han, P. Du, W. Lai and R. Cao, *Phys. Chem. Chem. Phys.*, 2014, **16**, 1883–1893.
50 A. Mahammed, B. Mondal, A. Rana, A. Dey and Z. Gross, *Chem. Commun.*, 2014, **50**, 2725–2727.
51 B. Mondal, K. Sengupta, A. Rana, A. Mahammed, M. Botoshansky, S. G. Dey, Z. Gross and A. Dey, *Inorg. Chem.*, 2013, **52**, 3381–3387.
52 H. Lei, H. Fang, Y. Han, W. Lai, X. Fu and R. Cao, *ACS Catal.*, 2015, **5**, 5145–5153.
53 D. L. Dubois, *Inorg. Chem.*, 2014, **53**, 3935–3960.
54 V. S. Thoi, Y. Sun, J. R. Long and C. J. Chang, *Chem. Soc. Rev.*, 2013, **42**, 2388–2400.
55 P. Wang, G. Liang, C. E. Webster and X. Zhao, *Eur. J. Inorg. Chem.*, 2020, **2020**, 3534–3547.
56 J. A. Cracknell, K. A. Vincent and F. A. Armstrong, *Chem. Rev.*, 2008, **108**, 2439–2461.
57 W. Lubitz, H. Ogata, O. Rüdiger and E. Reijerse, *Chem. Rev.*, 2014, **114**, 4081–4148.
58 A. Adamska-Venkatesh, D. Krawietz, J. Siebel, K. Weber, T. Happe, E. Reijerse and W. Lubitz, *J. Am. Chem. Soc.*, 2014, **136**, 11339–11346.
59 Y. Nicolet, A. L. De Lacey, X. Vernède, V. M. Fernandez, E. C. Hatchikian and J. C. Fontecilla-Camps, *J. Am. Chem. Soc.*, 2001, **123**, 1596–1601.
60 R. Tatematsu, T. Inomata, T. Ozawa and H. Masuda, *Angew. Chemie Int. Ed.*, 2016, **55**, 5247–5250.
61 A. D. Wilson, R. H. Newell, M. J. McNevin, J. T. Muckerman, M. R. DuBois and D. L. DuBois, *J. Am. Chem. Soc.*, 2006, **128**, 358–366.
62 M. Fang, E. S. Wiedner, W. G. Dougherty, W. S. Kassel, T. Liu, D. L. Dubois and R. M. Bullock, *Organometallics*, 2014, **33**, 5820–5833.
63 A. Dutta, S. Lense, J. Hou, M. H. Engelhard, J. A. S. Roberts and W. J. Shaw, *J. Am. Chem. Soc.*, 2013, **135**, 18490–18496.
64 K. E. Clary, M. Karayilan, K. C. McCleary-Petersen, H. A. Petersen, R. S. Glass, J. Pyun and D. L. Lichtenberger, *Proc. Natl. Acad. Sci. U. S. A.*, 2020, **117**, 32947–32953.
65 W. P. Brezinski, M. Karayilan, K. E. Clary, N. G. Pavlopoulos, S. Li, L. Fu, K. Matyjaszewski, D. H. Evans, R. S. Glass, D. L. Lichtenberger, J. Pyun, P. Brezinski, M. Karayilan, K. E. Clary, N. Avlopoulos, R. S. Glass, D. L. Lichtenberger, J. Pyun, S. Li, L. Fu, K. Matyjaszewski and D. H. Evans, *Angew. Chemie Int. Ed.*, 2018, **57**, 11898–11902.
66 C. H. Lee, D. K. Dogutan and D. G. Nocera, *J. Am. Chem. Soc.*, 2011, **133**, 8775–8777.
67 M. M. Roubelakis, D. K. Bediako, D. K. Dogutan and D. G. Nocera, *Energy Environ. Sci.*, 2012, **5**, 7737–7740.
68 D. K. Bediako, B. H. Solis, D. K. Dogutan, M. M. Roubelakis, A. G. Maher, C. H. Lee, M. B. Chambers, S. Hammes-Schiffer and D. G. Nocera, *Proc. Natl. Acad. Sci. U. S. A.*, 2014, **111**, 15001–15006.
69 J. M. Camara and T. B. Rauchfuss, *Nat. Chem.*, 2012, **4**, 26–30.
70 J. M. Le, G. Alachouzos, M. Chino, A. J. Frontier, A. Lombardi and K. L. Bren, *Biochemistry*, 2020, **59**, 1289–1297.
71 J. L. Alvarez-Hernandez, A. E. Sopchak and K. L. Bren, *Inorg. Chem.*, 2020, **59**, 8061–8069.
72 J. L. Alvarez-Hernandez, J. W. Han, A. E. Sopchak, Y. Guo and K. L. Bren, *ACS Energy Lett.*, 2021, **6**, 2256–2261.
73 J. W. Wang, K. Yamauchi, H. H. Huang, J. K. Sun, Z. M. Luo, D. C. Zhong, T. B. Lu and K. Sakai, *Angew. Chemie Int. Ed.*, 2019, **58**, 10923–10927.
74 J. N. H. Reek, B. de Bruin, S. Pullen, T. J. Mooibroek, A. M. Kluwer and X. Caumes, *Chem. Rev.*, 2022, **122**, 12308–12369.
75 B. Sun, T. Yoshino, S. Matsunaga and M. Kanai, *Adv. Synth. Catal.*, 2014, **356**, 1491–1495.
76 P. Dahiya, A. Sarkar and B. Sundararaju, *Adv. Synth. Catal.*, 2022, **364**, 2642–2647.
77 P. Dahiya, M. K. Gangwar and B. Sundararaju, *ChemCatChem*, 2021, **13**, 934–939.
78 C. Sandford, M. A. Edwards, K. J. Klunder, D. P. Hickey, M. Li, K. Barman, M. S. Sigman, H. S. White and S. D. Minteer, *Chem. Sci.*, 2019, **10**, 6404–6422.
79 K. J. Lee, B. D. McCarthy and J. L. Dempsey, *Chem. Soc. Rev.*, 2019, **48**, 2927–2945.
80 D. H. Pool, M. P. Stewart, M. O'Hagan, W. J. Shaw, J. A. S. Roberts, R. M. Bullock and D. L. DuBois, *Proc. Natl. Acad. Sci. U. S. A.*, 2012, **109**, 15634–15639.
81 A. Dutta, S. Lense, J. Hou, M. H. Engelhard, J. A. S. Roberts and W. J. Shaw, *J. Am. Chem. Soc.*, 2013, **135**, 18490–18496.
82 C. P. Andrieux, J. M. Dumas-Bouchiat and J. M. Savéant, *J. Electroanal. Chem. Interfacial Electrochem.*, 1980, **113**, 1–18.
83 J. M. Saveant and E. Vianello, *Electrochim. Acta*, 1965, **10**, 905–920.
84 C. Tsay and J. Y. Yang, *J. Am. Chem. Soc.*, 2016, **138**, 14174–14177.
85 M. A. Gross, A. Reynal, J. R. Durrant and E. Reisner, *J. Am. Chem. Soc.*, 2014, **136**, 356–366.

86 M. Van Der Meer, E. Glais, I. Siewert, B. Sarkar, M. Van Der Meer, E. Glais, B. Sarkar and I. Siewert, *Angew. Chemie Int. Ed.*, 2015, **54**, 13792–13795.
87 L. Tensi and A. Macchioni, *ACS Catal.*, 2020, **10**, 7945–7949.
88 L. Tensi, L. Rocchigiani, G. Menendez Rodriguez, E. Mosconi, C. Zuccaccia, F. De Angelis and A. Macchioni, *Catal. Sci. Technol.*, 2023, **13**, 6743–6750.
89 M. L. Pegis, B. A. McKeown, N. Kumar, K. Lang, D. J. Wasylenko, X. P. Zhang, S. Raugei and J. M. Mayer, *ACS Cent. Sci.*, 2016, **2**, 850–856.
90 D. J. Martin, C. F. Wise, M. L. Pegis and J. M. Mayer, *Acc. Chem. Res.*, 2020, **53**, 1056–1065.
91 Y. H. Wang, B. Mondal and S. S. Stahl, *ACS Catal.*, 2020, **10**, 12031–12039.
92 B. D. Groff and J. M. Mayer, *ACS Catal.*, 2022, **12**, 11692–11696.
93 K. Teindl, B. O. Patrick and E. M. Nichols, *J. Am. Chem. Soc.*, 2023, **145**, 17176–17186.
94 M. Langerman, P. H. van Langevelde, J. J. van de Vijver, M. A. Siegler and D. G. H. Hetterscheid, *Inorg. Chem.*, 2023, **62**(48), 19593–19602.
95 J. L. Alvarez-Hernandez, A. E. Sopchak and K. L. Bren, *Inorg. Chem.*, 2020, **59**, 8061–8069.
96 K. E. Clary, M. Karayilan, K. C. McCleary-Petersen, H. A. Petersen, R. S. Glass, J. Pyun and D. L. Lichtenberger, *Proc. Natl. Acad. Sci. U. S. A.*, 2020, **117**(52), 32947–32953.
97 J. L. Alvarez-Hernandez, J. Won Han, A. E. Sopchak, Y. Guo and K. L. Bren, *ACS Energy Lett.*, 2022, **6**(6), 2256–2261.
98 R. Custelcean and J. E. Jackson, *Chem. Rev.*, 2001, **101**, 1963–1980.
99 R. H. Crabtree, *Science*, 1998, **282**, 2000–2001.

